

I κ B kinase α is required for development and progression of *KRAS*-mutant lung adenocarcinoma

Malamati Vreka^{1,2,6}, Ioannis Lilis^{1,6}, Maria Papageorgopoulou^{1,2,6}, Georgia A. Giotopoulou^{1,2}, Marina Lianou¹, Ioanna Giopanou¹, Nikolaos I. Kanellakis¹, Magda Spella¹, Theodora Agalioti¹, Vasileios Armenis¹, Torsten Goldmann³, Sebastian Marwitz³, Fiona E. Yull⁴, Timothy S. Blackwell⁴, Manolis Pasparakis⁵, Antonia Marazioti^{1,7*}, and Georgios T. Stathopoulos^{1,2,7*}

¹ *Laboratory for Molecular Respiratory Carcinogenesis, Department of Physiology; Faculty of Medicine, University of Patras; Rio, Achaia, 26504; Greece.*

² *Comprehensive Pneumology Center (CPC) and Institute for Lung Biology and Disease (iLBD); University Hospital, Ludwig-Maximilians University and Helmholtz Zentrum München, Member of the German Center for Lung Research (DZL); Munich, Bavaria, 81377; Germany.*

³ *Clinical and Experimental Pathology, Research Center Borstel; Airway Research Center North (ARCN), Member of the German Center for Lung Research (DZL); Borstel, 23845, Germany.*

⁴ *Department of Medicine, Division of Allergy, Pulmonary and Critical Care Medicine; Vanderbilt University School of Medicine; Nashville, TN, 37240; USA.*

⁵ *Mouse Genetics and Inflammation Laboratory, Institute for Genetics, University of Cologne; Cologne, 50931, Germany.*

⁶ *Co-first authors.*

⁷ *Co-senior authors*

*** Corresponding Authors to whom requests for reprints and correspondence should be addressed:** Georgios T. Stathopoulos (gstathop@upatras.gr) and Antonia Marazioti (amarazioti@upatras.gr); Faculty of Medicine, University of Patras; 1 Asklepiou Str., University Campus, 26504 Rio, Greece; Phone: +302610969154; Fax: +302610969176.

Financial Support: This work was supported by European Research Council 2010 Starting Independent Investigator and 2015 Proof of Concept Grants (260524 and 679345, respectively, awarded to G.T. Stathopoulos), as well as a Research Award by the Hellenic Thoracic Society (awarded to M. Vreka).

Running Title: IKK α in lung adenocarcinoma.

Key words: NF- κ B; *CHUK*; urethane; bioluminescence; non-oncogene addiction.

Precis: Findings report a novel requirement for IKK α in mutant *KRAS* lung tumor formation with potential therapeutic applications.

Total word count: 4,473

Total number of figures: 7

References: 50

Conflict of interest: The authors declare no conflicts of interest.

ABSTRACT

Although oncogenic activation of nuclear factor (NF)- κ B has been identified in various tumors, the NF- κ B-activating kinases (inhibitor of NF- κ B kinases, IKK) responsible for this are elusive. In this study, we determined the role of IKK α and IKK β in *KRAS*-mutant lung adenocarcinomas induced by the carcinogen urethane and by respiratory epithelial expression of oncogenic *KRAS*^{G12D}. Using NF- κ B reporter mice and conditional deletions of IKK α and IKK β , we identified two distinct early and late activation phases of NF- κ B during chemical and genetic lung adenocarcinoma development, which were characterized by nuclear translocation of *RelB*, I κ B β , and IKK α in tumor-initiated cells. IKK α was a cardinal tumor promoter in chemical and genetic *KRAS*-mutant lung adenocarcinoma, and respiratory epithelial IKK α -deficient mice were markedly protected from the disease. IKK α specifically cooperated with mutant *KRAS* for tumor induction in a cell-autonomous fashion, providing mutant cells with a survival advantage *in vitro* and *in vivo*. IKK α was highly expressed in human lung adenocarcinoma, and a heat shock protein 90 inhibitor that blocks IKK function delivered superior effects against *KRAS*-mutant lung adenocarcinoma compared with a specific IKK β inhibitor. These results demonstrate an actionable requirement for IKK α in *KRAS*-mutant lung adenocarcinoma, marking the kinase as a therapeutic target against this disease.

INTRODUCTION

Tumors harboring mutations in the V-Ki-ras2 Kirsten rat sarcoma viral oncogene homolog (*KRAS*) are notoriously resistant to current treatments (1). Lung adenocarcinoma (LADC), the number one cancer killer worldwide (2), harbors *KRAS* mutations in up to 30-40% of the cases diagnosed in Europe and North America (3). A cardinal mechanism of *KRAS* mutation-associated drug resistance appears to be the oncogene's addiction to transcriptional programs that facilitate sustained tumor-initiated cell survival, such as nuclear factor (NF)- κ B (4). To this end, mutant *KRAS* was recently shown to interact with NF- κ B-activating kinases [inhibitor of NF- κ B (I κ B) kinases, IKKs] to promote cancer cell survival, stemness, and drug resistance (5, 6).

NF- κ B is activated via the canonical (involving I κ B α , IKK β , and *RelA/P50*) and non-canonical (comprising I κ B β , IKK α , and *RelB/P52*) pathways (7). We and others previously documented NF- κ B activation in murine and human LADC (8-10). However, the IKKs responsible for this remain elusive, and most studies focused on IKK β , IKK ϵ , and TANK-binding kinase 1 (TBK1; 11-14). IKK α participates in both canonical and non-canonical NF- κ B pathways, and co-operates with IKK β for tumor cell growth *in vitro* (11, 15), but its role in LADC development *in vivo* is uncharted.

We deployed NF- κ B reporter and conditional IKK α and IKK β -deleted mice to decipher the timing of NF- κ B activation and the mutual impact of IKK α and IKK β on LADC development. In mouse models of tobacco carcinogen- and oncogenic *KRAS*^{G12D}-triggered LADC, IKK α was cardinal for disease initiation and progression. Moreover, IKK α selectively fostered cellular proliferation in the context of mutant *KRAS*, and was also highly expressed in human LADC.

Importantly, dual IKK α / IKK β inhibition yielded promising results against *KRAS*-driven LADC, lending hope for translational applications of our findings.

MATERIALS AND METHODS

Additional Methods are described in the Online Supplement.

Mice: *C57BL/6J* (#000664), *FVB/NJ* (#001800), B6.129(Cg)-*Gt(ROSA)26Sor^{tm4(ACTB-tdTomato,-EGFP)LoxP/J}* (*mT/mG*; #007676; 16), B6.129S4-*Kras^{tm4Tyj}/J* (LSL.KRAS^{G12D}; #008179; 17), NOD.CB17-*Prkdc^{<scid>}/J* (*NOD/SCID*; #001303), and FVB.129S6(B6)-*Gt(ROSA)26Sor^{tm1(Luc)Kael}/J* (*LSL.R26.Luc*; #005125; 18) mice were from Jackson Laboratories (Bar Harbor, ME). NF-κB reporter mice (*NGL*; NF-κB.GFP.Luciferase), B6.B4B6-*Chuk^{<tm1Mpa>/Cgn}* (*Chukff*), and B6.B4B6-*Ikkbb^{<tm2.1Mpa>/Cgn}* (*Ikkbbff*), B6;CBA-Tg(*Scgb1a1-cre*)1Vart/Flmg (*Scgb1a1.Cre*), and Tg(*Sftpc-cre*)1Blh (*Sftpc.Cre*) mice have been described (8, 19-21). Mice were bred >F9 to the *C57BL/6* and/or *FVB* backgrounds at the University of Patras Center for Animal Models of Disease. The number of mice used for these studies ($n = 542$) is detailed in Supplementary Table S1.

Reagents: Urethane (CAS#51-79-6) and 3-(4,5-dimethylthiazol-2-yl)-2,5-diphenyltetrazolium bromide (MTT) assay were from Sigma (St. Louis, MO), adenoviruses from the Vector Development Lab of the Baylor College of Medicine (Houston, TX), D-luciferin from Gold Biotechnology (St. Louis, MO), HEK293T cells from ATCC (Wesel, Germany), and Lewis lung carcinoma (LLC) and A549 lung adenocarcinoma cells from the NCI Tumor Repository (Frederick, MD). Primers and antibodies are listed in Supplementary Tables S2 and S3. Lentiviral shRNA pools (Santa Cruz, Dallas, TX) are described in Supplementary Table S4.

Mouse models of LADC. Chemical-induced LADC was induced in *FVB* and *C57BL/6* mice, respectively, by a single or by ten consecutive weekly intraperitoneal exposures to 1 g/Kg

urethane (8, 22-24). *KRAS*^{G12D}-driven LADC was induced via intratracheal injections of 5×10^8 plaque-forming units (PFU) adenovirus type 5 encoding CRE recombinase (Ad-*Cre*) to *LSL.KRAS*^{G12D} mice on the *C57BL/6* background (9, 17). *NOD/SCID* and *C57BL/6* mice were anesthetized by isoflurane and received 2×10^6 HEK293T and 0.5×10^6 tumor cells into the rear flank and vertical tumor diameters (δ) were measured and mice were imaged for bioluminescent detection of cell mass weekly thereafter. Cell spot volume (V) was calculated as $V = \pi \times (\delta_1 \times \delta_2 \times \delta_3) / 6$, and mice were killed after six weeks. Flank tumors were harvested and fixed with 4% paraformaldehyde or processed for immunoblotting.

Drug treatments. *LSL.KrasG12D;LSL.R26.Luc* mice received 5×10^8 PFU intratracheal Ad-*Cre* followed by daily intraperitoneal injections of 100 μ L saline or 0.5 mg/Kg TPCA-1 or 17-DMAG in 100 μ L saline at days 14-28 or 84-112 post-Ad-*Cre*. Mice were imaged for bioluminescent detection of LADC burden at 0, 14, 28, 84, and 112 days post-Ad-*Cre*. Mice were sacrificed and lungs were harvested at 112 days post-Ad-*Cre*.

Cellular Assays. Mouse primary lung adenocarcinoma cells and airway epithelial cells were derived from the lungs of urethane (single dose 1 g/Kg) or saline-treated *FVB* or *C57BL/6* mice by simple tumor or large airway dissection or epithelial stripping, respectively, and 5-month or 5-day culture, respectively, as described elsewhere (25). These cell lines were named XYLA# with X signifying the mouse strain (F, *FVB*; C, *C57BL/6*), Y the carcinogen used (U, urethane), LA lung adenocarcinoma, and # their serial number by derivation date. Cells were cultured at 37°C in 5% CO₂-95% air using DMEM supplemented with 10% FBS, 2mM L-glutamine, 1 mM pyruvate, 100 U/ml penicillin, and 100mg/ml streptomycin. Cells were tested biannually for identity (by the short tandem repeat method) and for *Mycoplasma Spp.* (by PCR). For

experiments, frozen cells were reconstituted and were passaged 2-5 times for less than two weeks. *In vitro* cancer cell proliferation was determined using the 3-(4,5-dimethylthiazol-2-yl)-2,5-diphenyltetrazolium bromide (MTT) assay. For this, 2×10^4 cells/well were plated onto 96-well plates. Daily thereafter, 15 μ L of 5 mM MTT working solution in PBS was added to wells to be measured that day. The plate was incubated for 4 h at 37 °C in a 5% CO₂ humidified incubator followed by addition of 100 μ L acidified isopropanol per well for sediment solubilization and absorbance measurement at 492 nm on a MR-96A photometer (Mindray, Shenzhen, China). For soft agar colony formation assay, 7.5×10^3 cells were plated in 60 mm culture vessels in semi-solid 0.7% agarose in full culture medium and were incubated for 30 days at 37 °C in a 5% CO₂ humidified incubator. 2 mL fresh culture medium was added to each vessel biweekly. After incubation, 500 μ L MTT working solution was added to each vessel and plates were dried, inverted, photographed, and colonies were counted, as described elsewhere (25).

Human samples. Matched tumor and normal lung tissue RNA and sections of 23 and 35, respectively, previously reported patients with LADC from Institution 3 were used for microarray and immunohistochemistry for IKK α and IKK β (26). Human studies were approved a priori by the ethics committee of the University of Lübeck, Germany (approval # AZ 12-220) and were conducted according to the Declaration of Helsinki. Written informed consent was obtained from all patients. IKK score was 0, 1, 2, or 3 for no, cytoplasmic only, cytoplasmic and nuclear, and nuclear only immunoreactivity, respectively (modified from 11).

Statistics. Sample size (n ; always biological) was determined using G*power (<http://www.gpower.hhu.de/>), assuming $\alpha = 0.05$, $\beta = 0.05$, and $d = 1.5$. Data were acquired by two blinded readers, reevaluated if >20% deviant (no data were excluded), examined for

normality by Kolmogorov-Smirnov test, and presented as median (interquartile range) or mean \pm SEM. Differences in frequencies were examined by Fischer's exact/ χ^2 tests, in means of normally distributed variables by t-test or one-way ANOVA/Bonferroni post-tests, and in medians of non-normally distributed variables by Mann-Whitney test or Kruskal-Wallis/Dunn's post-tests. Survival and flank tumor volume were examined by Kaplan-Meier estimates/log-rank tests and two-way ANOVA/Bonferroni post-tests. Probability (P) is two-tailed; $P < 0.05$ was considered significant. Statistics and plots were done on Prism v5.0 (GraphPad, La Jolla, CA).

Study approval. All animal experiments were approved a priori by the Veterinary Administration of Western Greece according to a full and detailed protocol (approval # 276134/14873/2). Male and female mice were sex-, weight (20-25 g)-, and age (6-12 week)-matched. Human studies were approved *a priori* by the ethics committee of the University of Lübeck, Germany (approval # AZ 12-220).

RESULTS

NF- κ B is activated in *KRAS*-mutant LADC.

To map pulmonary NF- κ B activity during *KRAS*-driven neoplasia, NF- κ B reporter mice (*NGL*) on the carcinogen-susceptible *FVB* background expressing NF- κ B-driven *Photinus Pyralis* luciferase (LUC) in-frame with EGFP (8, 23) received a single intraperitoneal injection of saline or the tobacco carcinogen urethane (1g/Kg) and were serially imaged for bioluminescence. Urethane causes respiratory epithelial *Kras*^{G12V/Q61R} mutations and progressive inflammation, hyperplasias, adenomas, and adenocarcinomas in *FVB* mice (22-25) that in this experiment also expressed the *NGL* reporter (Figs. 1A, B). In addition to the baseline signals of these mice, markedly increased light emission from the chest was exclusively detected in urethane-treated mice at early and late time-points corresponding to carcinogen-induced inflammation and LADC, respectively (8). Enhanced NF- κ B activation indicated by the EGFP reporter emanated exclusively from LADC (Figs. 1C-F). In a second approach, *NGL* mice were intercrossed with mice carrying a conditional loxP-STOP-loxP.*KRAS*^{G12D} allele (*LSL.KRAS*^{G12D}; 17), and *NGL* and *NGL;LSL.KRAS*^{G12D} offspring (all *C57BL/6* background) received intratracheal Ad-*Cre* and were longitudinally imaged. In *LSL.KRAS*^{G12D} mice, progressive inflammation, hyperplasia, adenomas, and adenocarcinomas carrying the *KRAS* mutation are inflicted by Ad-*Cre* (9, 17). To titrate Ad-*Cre*, *mT/mG* CRE-reporters that switch from membranous Tomato (mT) to EGFP (mG) fluorescence upon CRE-recombination (16), received 0, 5 x 10⁷, 5 x 10⁸, or 5 x 10⁹ PFU intratracheal Ad-*Luc* or Ad-*Cre* and were killed upon subsidence of transient Ad-mediated transgene expression at two weeks post-injection (27). The low, intermediate, and high Ad-*Cre* titers, respectively, caused infrequent, stochastic, and ubiquitous respiratory epithelial

recombination (Supplementary Figs. S1A, B). We selected 5×10^8 PFU Ad-*Cre* to stochastically induce recombination into the respiratory epithelium of *NGL* and *NGL;LSL.KRAS^{G12D}* mice (Supplementary Fig. S1C). Similar to the urethane model, two phases of enhanced chest light emission by *NGL;LSL.KRAS^{G12D}* but not *NGL* mice were observed, coinciding with early inflammation and late LADC development (8, 22-24, 28). Again, NF- κ B-dependent EGFP expression was confined to LADC (Supplementary Figs. S1D-S1G). These data demonstrate biphasic pulmonary NF- κ B activation during *KRAS*-driven LADC development.

***KRAS*-mutant LADC displays both canonical and non-canonical NF- κ B activity.**

To investigate the NF- κ B pathway at play during *KRAS*-mutant inflammation, hyperproliferation, and LADC formation, the immunoreactivity of nuclear and cytoplasmic protein extracts of whole lungs of urethane-treated *FVB* mice and of Ad-*Cre*-treated *LSL.KRAS^{G12D}* mice for NF- κ B subunits, kinases, and inhibitors were probed longitudinally (Figs. 2A-D). In the urethane model, marked RelB and RelA immunoreactivity was detected in nuclear extracts and enhanced I κ B α , I κ B β , IKK α , IKK β , and TBK1 immunoreactivity in cytoplasmic extracts of the neoplastic stage. Some immunoreactivity was also present in early stages but their expression peaked in tumor-bearing lungs, while no IKK ϵ signal was evident at any time-point. In the *LSL.KRAS^{G12D}* model, enhanced nuclear RelB and P52 and modest RelA immunoreactivity was detected in nuclear extracts of tumor bearing lungs, together with some cytoplasmic immunoreactivity for I κ B β , IKK α , and TBK1 (120 days). In addition, some RelA, RelB, P52, I κ B α , I κ B β , and TBK1 immunoreactivity was evident in same-day-treated lungs (0 days), some RelA, RelB, P52, IKK α , and TBK1 immunoreactivity in inflammatory and proliferative lungs (30 and 60 days), and no IKK β and IKK ϵ signal at any stage. IKK expression patterns were

corroborated using immunofluorescent detection of IKK α /IKK β on lung sections of urethane-treated *FVB* and Ad-*Cre*-treated *LSL.KRAS*^{G12D} mice at 240 and 120 days post-treatment, respectively. In both models, IKK α was expressed by a significant proportion of LADC cells, while minimal IKK β expression was detectable (Figs. 2E, F). To further characterize NF- κ B activity of LADC, LADC cells were derived from the lungs of saline and urethane-treated *FVB* mice, according to established methods (Supplementary Figs. S2A,B; 25, 29). LADC cells exhibited enhanced nuclear *RelB* (but not *RelA*) localization and activity compared with saline- and urethane-treated lungs (Supplementary Figs. S2C,D). Taken together, these results indicate co-activation of the canonical and non-canonical NF- κ B pathways in LADC.

Respiratory epithelial IKK α promotes *KRAS*-driven LADC.

We next functionally assessed the role of IKK α and IKK β in LADC development, utilizing conditional IKK α and IKK β gene-deleted mice (*Chuk1^{fl/fl}* and *Ikkb1^{fl/fl}*) that feature loxP-flanked alleles excised upon CRE expression (19). In a first line of experiments, *mT/mG* CRE-reporter (control), *Chuk1^{fl/fl}*, and *Ikkb1^{fl/fl}* mice on the urethane-resistant *C57BL/6* background (8) received 5×10^9 PFU intratracheal Ad-*Cre* (a titer causing recombination in ~75% of the respiratory epithelium within two weeks; Supplementary Figs. S1A, B), and were started two weeks thereafter on ten weekly doses of 1g/kg intraperitoneal urethane, a regimen that reproducibly induces LADC in *C57BL/6* mice (23, 29). In this multi-hit model, stochastic *KRAS* mutations, inflammation, apoptosis, and regeneration were repeatedly inflicted across IKK-deleted and non-deleted respiratory epithelium (Fig. 3A). Interestingly, *Ikkb1^{fl/fl}* mice displayed decreased survival during repeated urethane exposures, suggesting a role for IKK β in epithelial repair (Fig. 3B). However, at six months post-urethane start, IKK α -deleted mice had markedly decreased

LADC incidence, multiplicity, and burden per lung compared with controls, while IKK β -deleted mice displayed only minor reductions in tumor multiplicity but not burden (Figs. 3C-G). These experiments were replicated on *Chukfff* and *Ikkkbfff* mice back-crossed >F9 to the single-hit *FVB* model that recapitulates the mutation spectrum of human LADC and allows separate insights into the effects of IKK deletion on tumor initiation and progression via observations on LADC number and size after six months (8, 22-24). For this, *WT* control, *Chukfff*, and *Ikkkbfff* mice (all *FVB*) received 5×10^9 PFU intratracheal Ad-*Cre*, followed by a single intraperitoneal exposure to 1g/kg urethane (Supplementary Fig. S3A). All genotypes comparably survived single-hit urethane (Supplementary Fig. S3B). Again, *Chukfff* mice developed fewer and smaller LADC compared with controls, indicating marked tumor-initiating and promoting effects of IKK α , but *Ikkkbfff* mice displayed tumor incidence, number, size, and load closely resembling *WT* littermates, suggesting that the minor tumor-promoting effects of IKK β require repetitive carcinogen challenge to become evident (Supplementary Figs S3C-G). *Chukfff* and *Ikkkbfff* mice were also intercrossed with *Scgb1a1.Cre* (20) and *Sftpc.Cre* (21) CRE-drivers (all *C57BL/6*) and their offspring received ten consecutive weekly intraperitoneal injections of 1 g/Kg urethane starting at six weeks of age (Supplementary Fig. S4A). Interestingly, both *Scgb1a1.Cre* and *Sftpc.Cre*-driven IKK α -deletion was equally protective against LADC, while IKK β -deletion had no effect (hence pooled *Scgb1a1.Cre* and *Sftpc.Cre* data are presented; Supplementary Figs. S4B-E). To solidify the link between IKK α and mutant *KRAS* and to discriminate between cell-autonomous and paracrine IKK α effects, *Chukfff* and *Ikkkbfff* mice were intercrossed with *LSL.KRAS^{G12D}* mice (all *C57BL/6*) and their offspring received 5×10^8 PFU intratracheal Ad-*Cre*, a model where *KRAS^{G12D}*-expression and IKK-deletion coincide (Fig. 4A). Lung morphometry (30) at four months post-Ad-*Cre* showed that IKK α -deleted mice had markedly

decreased LADC burden compared with controls, while IKK β -deleted mice displayed an intermediate phenotype (Figs. 4B-E). Collectively these findings show that IKK α promotes *KRAS*-mutant LADC in a cell-autonomous fashion, independent from and more pronounced than IKK β .

IKK α selectively fosters *KRAS*-mutant cell prevalence *in vitro* and *in vivo*.

We next stably transfected HEK293T benign human embryonic kidney cells with vectors encoding control random sequence (pC), RFP (pRFP), EGFP (peGFP), wild-type (peGFP.*Kras*^{WT}) or mutant (peGFP.*Kras*^{G12C}) murine *Kras* in-frame with EGFP, and murine IKK α (pChuk) or IKK β (pIkkbb) in various combinations. After transgene expression was validated, RFP-expressing control cells and EGFP-expressing intervention cells co-transfected with various combinations of peGFP.*Kras*^{WT}/ peGFP.*Kras*^{G12C} and pChuk/pIkkbb were mixed at equal ratios and co-cultured for one week, followed by quantification by fluorescent microscopy and flow cytometry (Supplementary Figs. S5A, B). Of note, as opposed to successful pIkkbb co-expression with peGFP.*Kras*^{WT}, pIkkbb co-expression with peGFP.*Kras*^{G12C} was repeatedly impossible ($n = 5$), indicating mutual repulsion of mutant *Kras*^{G12C} and IKK β , similar to what was previously observed with other RAS/I κ B-like GTPases called κ B-RAS (Supplementary Fig. S5B; 31). Despite this, IKK β provided a proliferative advantage to HEK293T cells expressing *Kras*^{WT}, whereas *Kras*^{G12C}-expressing HEK293T cells proliferated more efficiently upon IKK α overexpression (Supplementary Figs. S5C, D). Subsequently, HEK293T cells were stably transfected with pCAG.*Luc* followed by various combinations of pC, peGFP.*Kras*^{WT}, peGFP.*Kras*^{G12C}, pChuk, and/or pIkkbb, were validated, and two million cells were injected at different dorsal skin spots of *NOD/SCID* mice followed by serial spot volume assessment and

bioluminescence imaging. Again, IKK β boosted *in vivo* growth of HEK293T cells expressing *Kras*^{WT}, while *Kras*^{G12C}-expressing HEK293T cells were rendered more tumorigenic upon IKK α overexpression (Figs. 5A-C). Interestingly, none of eight *NOD/SCID* mice bearing subcutaneous *Kras*^{WT} cells developed pulmonary lesions, while five of eight mice with subcutaneous *Kras*^{G12C} cells developed lung metastases ($P = 0.0256$, χ^2 test; Fig. 5D). We next examined HEK293T spots that had grown into tumors for NF- κ B pathway component immunoreactivity. By immunoblotting, we observed nuclear localization of IKK α but not IKK β in control tumors expressing *Kras*^{WT} that was further enhanced by co-expression of IKK β . *Kras*^{G12C} tumors showed both IKK α and IKK β nuclear immunoreactivity, while *Kras*^{G12C}-IKK α -expressing tumors had enhanced IKK α and diminished IKK β nuclear signals, and *Kras*^{G12C}-IKK β -expressing tumors displayed loss of both nuclear signals (Fig. 5E). The nuclear localization of IKK α in *Kras*^{G12C}-IKK α co-expressing tumors was also evident on tissue sections by immunofluorescence (Fig. 5F). In addition to KRAS-IKK co-expression in benign cells, we stably expressed shRNAs specifically targeting IKK α and IKK β transcripts (*Chuk* and *Ikkkb* respectively) in different lung adenocarcinoma cell lines [LLC, Lewis lung adenocarcinoma cells; and primary lung adenocarcinoma cells derived from urethane-induced lung tumors of *FVB* (FULA) and *C57BL/6* (CULA) mice] bearing wild-type *Kras*^{WT} (CULA cells), *Kras*^{G12C} (LLC cells), *Kras*^{Q61R} (FULA1 and FULA3 cells), or silenced *Kras*^{Q61R} (FULA3 cells stably expressing *shKras*) (25, 29). Interestingly, IKK α silencing resulted in decreased clonogenic capacity *in vitro* and decreased tumor growth *in vivo* specifically of *KRAS*-mutant tumor cells (Supplementary Figs. 6A-6C). Moreover, this effect was not obvious *in vitro*, in line with recent observations on the *in vivo*-restricted effects of the oncogene (32). Collectively, these results indicated selective

addition of mutant *KRAS* to *IKK α* during carcinogenesis, possibly via nuclear *IKK α* functions reported elsewhere (33, 34).

Combined targeting of *IKK α* /*IKK β* is effective against LADC.

We subsequently evaluated the therapeutic potential of our findings using cellular and animal systems tailored to non-invasively monitor tumor growth and NF- κ B activity. For this, three *KRAS*-mutant LADC cell lines (mouse primary LADC, *Kras*^{Q61R}; murine Lewis lung carcinoma, *Kras*^{G12C}; A549 human LADC, *KRAS*^{G12S}) were stably transfected with constitutive (*pCAG.Luc*) and NF- κ B-dependent (*pNGL*) LUC reporters, inducibility of the NF- κ B reporter was validated, and cells were treated with increasing concentrations of the selective *IKK β* inhibitor TPCA-1 {2-[(aminocarbonyl)amino]-5-[4-fluorophenyl]-3-thiophenecarboxamide; 35) or the heat shock protein 90 (HSP90) inhibitor 17-DMAG (alvespimycin; 17-dimethylaminoethylamino-17-demethoxygeldanamycin; 36, 37) that blocks, among other targets, *IKK α* and *IKK β* function; bioluminescence imaging of live *pCAG.Luc* cells after 48-hour treatments was used to determine cell killing and of *pNGL* cells after 4-hour treatments NF- κ B inhibition. Intriguingly, 17-DMAG displayed superior efficacy in halting cell proliferation and NF- κ B activity in all three cell lines compared with TPCA-1, as evident by 4-5-fold lower 50% inhibitory concentrations of *pCAG.Luc* activity (mean \pm SD: 28 \pm 12 μ M for 17-DMAG and 114 \pm 30 for TPCA-1) and 200-1000-fold lower 50% inhibitory concentrations of *pNGL* activity (mean \pm SD: 0.133 \pm 0.068 μ M for 17-DMAG and 62 \pm 30 for TPCA-1) (Supplementary Figs. S7A-S7E). Based on these results and the data from *NGL* mice with *KRAS*^{G12D} tumors (Supplementary Fig. S1), we designed an *in vivo* study where mice with *KRAS*^{G12D}-mutant LADCs received low doses of either drug tailored to inhibit NF- κ B activity rather than cell proliferation in both preventive and curative modes. To

enable repetitive non-invasive bioluminescent quantification of tumor burden *in vivo*, mice harboring a conditional loxP-STOP-loxP.*R26.Luc* allele (*LSL.R26.Luc*; 18) were intercrossed with *LSL.KRAS^{G12D}* mice (17; all *C57BL/6*), yielding a model where CRE-recombination leads to simultaneous *KRAS^{G12D}* and LUC expression (Fig. 6A; 38). *LSL.KRAS^{G12D};LSL.R26.Luc* mice ($n = 30$) received 5×10^8 intratracheal PFU Ad-*Cre* and were allocated to drug treatments during the two distinct phases of NF- κ B activation identified from *LSL.KRAS^{G12D};NGL* mice (Supplementary Fig. S1): between days 14-28 post-Ad-*Cre* (prevention trial) or between days 84-112 post-Ad-*Cre* (regression trial; Fig. 6B). Treatments consisted of 100 μ L daily intraperitoneal saline, TPCA-1, or 17-DMAG, both at 0.5 mg/Kg in 100 μ L saline, equivalent by body volume extrapolation to maximal *in vivo* concentrations of 1.79 μ M for TPCA-1 and of 0.77 μ M for 17-DMAG, far inferior to cytotoxic concentrations (Supplementary Fig. S7). Bioluminescent detection of developing LADC revealed that TPCA-1 had no effect, while 17-DMAG prevention and regression regimens efficiently blocked tumor development compared with controls (Figs. 6C, D). Collectively, these results indicate that 17-DMAG exerts beneficial effects against *KRAS*-mutant LADCs *in vitro* and *in vivo*, even at low doses tailored to inhibit NF- κ B. On the contrary, a specific IKK β inhibitor failed to show any effect, further supporting a druggable addiction of IKK α with mutant *KRAS* in LADC.

IKK α in human LADC.

The relevance of our findings with human LADC was subsequently addressed. For this, tumor and adjacent normal-appearing lung tissues of 23 patients with LADC were analyzed for *CHUK* and *IKBKB* expression by microarray and of another 35 patients from the same series for IKK α and IKK β by immune-labelling (26). *CHUK* mRNA was overrepresented in normal-appearing

and LADC tissue compared with *IKBKB* mRNA, while the levels of both were not different between normal-appearing and tumor tissue (Fig. 7A). However, using a modified NF- κ B scoring system that examines staining intensity and localization (10), IKK α protein was significantly overexpressed in LADC compared with both normal-appearing tissues and with IKK β (Figs. 7B, C), suggesting its possible involvement in the pathogenesis of human LADC.

DISCUSSION

We report an actionable requirement for IKK α in *KRAS*-mutant LADC. Using chemical and transgenic delivery of *KRAS* mutations to the respiratory tract in combination with NF- κ B reporter and conditional IKK-deleted mice we map the patterns of NF- κ B activation in the lungs and identify the critical role of IKK α . We show that IKK α drives LADC through cell-autonomous effects that are specifically exerted in the cellular context of mutant *KRAS*. These findings have implications for human disease, since IKK α is overexpressed in human LADC and oncogenic *KRAS*-IKK α addiction was annihilated by treatment with 17-DMAG.

The findings are novel and important on various counts. First, NF- κ B activity of *KRAS*-mutant LADC is charted in living mice and is shown to be activated early after *KRAS* mutation induction and late in established LADC. This pattern is in line with observations from smokers at risk for LADC that feature airway epithelial NF- κ B activation (39) and from patients with established LADC that display oncogenic NF- κ B activation (10). The results are consistent with the hypothesis that NF- κ B activation occurs together with field mutagenesis in the respiratory tract, persists in mutated cells, and reappears during clinical manifestation of late disease (40), bearing implications for NF- κ B-based therapy and prevention (Fig. 7D).

Second, non-canonical together with canonical NF- κ B pathway components are shown to be activated in *KRAS*-driven LADC. Canonical NF- κ B signaling is long known to be important in human and experimental LADC (8-10), but activity of the alternative pathway has not been described. This finding is in accord with our previous observations of enhanced *RelB* activity of tumor cells in human LADC (10) and suggests important roles for alternative NF- κ B signaling in *KRAS*-driven LADC.

Importantly, IKK α is identified as the critical kinase for oncogenic NF- κ B activation of *KRAS*-mutant LADC. IKK α deletion provided beneficial effects in four different mouse models of combined *KRAS*-driven carcinogenesis and IKK depletion from the respiratory epithelium. In addition, 17-DMAG protected mice from *KRAS*^{G12D}-driven LADC when given early (preventive treatment) or late (regression trial), while the IKK β blocker TPCA-1 did not. Although 17-DMAG likely suppresses a spectrum of targets broader than IKK α and IKK β (41), inclusively targeting IKK α utilizing even this non-specific approach provided superior overall effects in reducing tumor burden compared with IKK β -specific inhibition (Fig. 7E). We were the first to identify that indirect IKK β blockade via overexpression of dominant negative I κ B α protects mice from urethane-induced LADC (8), a finding thereafter recapitulated in *KRAS*^{G12D}-mutant (9), and tobacco-smoke-induced (14) LADC. Urethane-triggered LADCs were recently genomically characterized and shown to harbor *Kras*^{Q61R}/*Kras*^{G12V} mutations (22), similar to human LADC (42). Based on these findings and results from other tumor types, research and drug discovery focused on IKK β yielding proteasome and IKK β inhibitors (35, 43). However, these provide poor outcomes in human LADC (44) and cause resistance or paradoxical tumor promotion in animal LADC models via myeloid NF- κ B inhibition, secondary mutation development, and/or enhanced neutrophil-provided IL-1 β (23, 45, 46). In addition, recent evidence indicates that IKK β might not be the only kinase responsible for oncogenic NF- κ B activation of *KRAS*-mutant LADC (47). To this end, TBK1 emerged as a *KRAS* addiction partner, and was found to mediate EGFR-inhibitor resistance (5, 6), while IKK ϵ promoted tumorigenesis together with TBK1 (13). Only one study addressed the role of IKK α depletion together with IKK β in lung cancer cells *in vitro* and found both kinases to be important (11). Our results identify for the first time the

pivotal role of IKK α in *de novo* development of *KRAS*-mutant LADC *in vivo* and position the kinase as a marked therapeutic target.

Using *in vitro* and *in vivo* competition studies, we determine that IKK α selectively fosters the survival of *KRAS*-mutant cells and is therefore addicted to the oncogene, while IKK β promotes the survival and maintenance of non-mutated cells. We hypothesize that in a stochastically *KRAS*-mutated respiratory field, this opposing addiction of IKK α and IKK β to mutant and wild-type *KRAS*, respectively, would lead over time via clonal selection to *KRAS*-mutant LADCs with enhanced IKK α activity (Fig. 7D). This cell-autonomous model is supported by the results from *KRAS*^{G12D} mice (where IKK α was selectively deleted in *KRAS*-mutant cells) and from HEK293T cells (where IKK/*KRAS* combinations functioned similarly *in vitro* and *in vivo*), notwithstanding the possibility for autocrine IKK α -triggered cytokine networks identified elsewhere (48,49). To this end, IKK α localized to the nucleus of our murine LADCs, a phenomenon that could enhance gene transcription or repress oncogenes (33, 34). Nuclear IKK α was also present in human LADC, which displayed enhanced nuclear IKK α immunoreactivity. The proposed IKK α function to site-independently foster *KRAS*-mutant cells also emanates from tissue-restricted IKK-deletion studies where IKK α was critical in both airway and alveolar cells, a result of importance given the cellular and histologic diversity of human LADC (50).

Finally, a feasible approach for translation of the findings is explored. Treatment with 17-DMAG was tailored to target NF- κ B activation of *KRAS*-mutant LADC *in vitro* and was translated to a preclinical study, where it was well-tolerated and effective against LADC *in vivo*, both preventively and therapeutically. The efficacy of 17-DMAG and the inefficacy of TPCA-1 strengthen the proposed link between mutant *KRAS* and IKK α and open up new avenues for

therapy/prevention of *KRAS*-mutant LADC (1). In summary, we report a requirement for IKK α in *KRAS*-driven LADC, implicate IKK α as a *KRAS* non-oncogene addiction partner, and show that targeting IKK α may confer beneficial effects against a currently untreatable disease that is the number one cancer killer in the world.

ACKNOWLEDGEMENTS

The authors thank the University of Patras Center for Animal Models of Disease and Advanced Light Microscopy Cores for experimental support.

REFERENCES

1. Stephen AG, Esposito D, Bagni RK, McCormick F. Dragging Ras Back in the Ring. *Cancer Cell* 2014;25:272–281.
2. Global Burden of Disease Cancer Collaboration, Fitzmaurice C, Dicker D, Pain A, Hamavid H, Moradi-Lakeh M, MacIntyre MF, et al. The Global Burden of Cancer 2013. *JAMA Oncol* 2015;1:505-527.
3. Cancer Genome Atlas Research Network. Comprehensive molecular profiling of lung adenocarcinoma. *Nature* 2014;511:543-550.
4. Weinstein IB, Joe A. Oncogene addiction. *Cancer Res* 2008;68:3077–3080.
5. Barbie DA, Tamayo P, Boehm JS, Kim SY, Moody SE, Dunn IF, et al. Systematic RNA interference reveals that oncogenic KRAS-driven cancers require TBK1. *Nature* 2009;462:108-112.
6. Seguin L, Kato S, Franovic A, Camargo MF, Lesperance J, Elliott KC, et al. An integrin β -KRAS-RalB complex drives tumour stemness and resistance to EGFR inhibition. *Nat Cell Biol* 2014;16:457-468.
7. Luo JL, Kamata H, Karin M. IKK/NF-kappaB signaling: balancing life and death-a new approach to cancer therapy. *J Clin Invest* 2005;115:2625-2632.
8. Stathopoulos GT, Sherrill TP, Cheng DS, Scoggins RM, Han W, Polosukhin VV, et al. Epithelial NF-kappaB activation promotes urethane-induced lung carcinogenesis. *Proc Natl Acad Sci U S A* 2007;104:18514-18519.

9. Meylan E, Dooley AL, Feldser DM, Shen L, Turk E, Ouyang C, et al. Requirement for NF-kappaB signalling in a mouse model of lung adenocarcinoma. *Nature* 2009;462:104-107.
10. Giopanou I, Lilis I, Papaleonidopoulos V, Marazioti A, Spella M, Vreka M, et al. Comprehensive Evaluation of Nuclear Factor-kB Expression Patterns in Non-Small Cell Lung Cancer. *PLoS One* 2015;10:e0132527.
11. Bassères DS, Ebbs A, Cogswell PC, Baldwin AS. IKK is a therapeutic target in KRAS-Induced lung cancer with disrupted p53 activity. *Genes Cancer* 2014;5:41-55.
12. Bivona TG, Hieronymus H, Parker J, Chang K, Taron M, Rosell R, et al. FAS and NF-kB signaling modulate dependence of lung cancers on mutant EGFR. *Nature* 2011;471:523-526.
13. Duran A, Linares JF, Galvez AS, Wikenheiser K, Flores JM, Diaz-Meco MT, et al. The signaling adaptor p62 is an important NF-kappaB mediator in tumorigenesis. *Cancer Cell* 2008;13:343-354.
14. Takahashi H, Ogata H, Nishigaki R, Broide DH, Karin M. Tobacco smoke promotes lung tumorigenesis by triggering IKKbeta- and JNK1-dependent inflammation. *Cancer Cell* 2010;17:89-97.
15. Nottingham LK, Yan CH, Yang X, Si H, Coupar J, Bian Y, et al. Aberrant IKKalpha and IKKbeta cooperatively activate NF-kappaB and induce EGFR/AP1 signaling to promote survival and migration of head and neck cancer. *Oncogene* 2014;33:1135-1147.

16. Muzumdar MD, Tasic B, Miyamichi K, Li L, Luo L. A global double fluorescent Cre reporter mouse. *Genesis* 2007;45:593-605.
17. Jackson EL, Willis N, Mercer K, Bronson RT, Crowley D, Montoya R, et al. Analysis of lung tumor initiation and progression using conditional expression of oncogenic K-ras. *Genes Dev* 2001;15:3243-3248.
18. Safran M, Kim WY, Kung AL, Horner JW, DePinho RA, Kaelin WG Jr. Mouse reporter strain for noninvasive bioluminescent imaging of cells that have undergone Cre-mediated recombination. *Mol Imaging* 2003;2:297-302.
19. Luedde T, Heinrichsdorff J, de Lorenzi R, De Vos R, Roskams T, Pasparakis M. IKK1 and IKK2 cooperate to maintain bile duct integrity in the liver. *Proc Natl Acad Sci U S A* 2008;105:9733-9738.
20. Oikonomou N, Mouratis MA, Tzouveleki A, Kaffe E, Valavanis C, Vilaras G, et al. Pulmonary autotoxin expression contributes to the pathogenesis of pulmonary fibrosis. *Am J Respir Cell Mol Biol* 2012;47:566-574.
21. Okubo T, Knoepfler PS, Eisenman RN, Hogan BL. Nmyc plays an essential role during lung development as a dosage-sensitive regulator of progenitor cell proliferation and differentiation. *Development* 2005;132:1363-1374.
22. Westcott PM, Halliwill KD, To MD, Rashid M, Rust AG, Keane TM, et al. The mutational landscapes of genetic and chemical models of Kras-driven lung cancer. *Nature* 2015;517:489-492.
23. Karabela SP, Psallidas I, Sherrill TP, Kairi CA, Zaynagetdinov R, Cheng DS, et al. Opposing effects of bortezomib-induced nuclear factor- κ B inhibition on chemical lung carcinogenesis. *Carcinogenesis* 2012;33:859-867.

24. Karabela SP, Kairi CA, Magkouta S, Psallidas I, Moschos C, Stathopoulos I, et al. Neutralization of tumor necrosis factor bioactivity ameliorates urethane-induced pulmonary oncogenesis in mice. *Neoplasia* 2011;13:1143-1151.
25. Agalioti T, Giannou AD, Krontira AC, Kanellakis NI, Kati D, Vreka M, et al. Mutant KRAS promotes malignant pleural effusion formation. *Nat Commun* 2017;8:15205.
26. Marwitz S, Depner S, Dvornikov D, Merkle R, Szczygieł M, Müller-Decker K, et al. Downregulation of the TGFβ Pseudoreceptor BAMBI in Non-Small Cell Lung Cancer Enhances TGFβ Signaling and Invasion. *Cancer Res* 2016;76:3785-3801.
27. Stathopoulos GT, Sherrill TP, Han W, Sadikot RT, Yull FE, Blackwell TS, et al. Host nuclear factor-kappaB activation potentiates lung cancer metastasis. *Mol Cancer Res* 2008;6:364-671.
28. Nikitin AY, Alcaraz A, Anver MR, Bronson RT, Cardiff RD, Dixon D, et al. Classification of proliferative pulmonary lesions of the mouse: recommendations of the mouse models of human cancers consortium. *Cancer Res* 2004;64:2307- 2316.
29. Giopanou I, Lilis I, Papaleonidopoulos V, Agalioti T, Kanellakis NI, Spiropoulou N, et al. Tumor-derived osteopontin isoforms cooperate with TRP53 and CCL2 to promote lung metastasis. *Oncoimmunology* 2017;6:e1256528.
30. Hsia CC, Hyde DM, Ochs M, Weibel ER; *ATS/ERS Joint Task Force on Quantitative Assessment of Lung Structure*. An official research policy statement of the American Thoracic Society/European Respiratory Society: standards for quantitative assessment of lung structure. *Am J Respir Crit Care Med* 2010;181:394-418
31. Chen Y, Vallee S, Wu J, Vu D, Sondek J, Ghosh G. Inhibition of NF-kappaB activity by IkappaBbeta in association with kappaB-Ras. *Mol Cell Biol* 2004;24:3048-3056.

32. Janes MR, Zhang J, Li LS, Hansen R, Peters U, Guo X, et al. Targeting KRAS Mutant Cancers with a Covalent G12C-Specific Inhibitor. *Cell* 2018;172:578-589.
33. Anest V, Hanson JL, Cogswell PC, Steinbrecher KA, Strahl BD, Baldwin AS. A nucleosomal function for IkappaB kinase-alpha in NF-kappaB-dependent gene expression. *Nature* 2003;423:659-663.
34. Yamamoto Y, Verma UN, Prajapati S, Kwak YT, Gaynor RB. Histone H3 phosphorylation by IKK-alpha is critical for cytokine-induced gene expression. *Nature* 2003;423:655-659.
35. Birrell MA, Hardaker E, Wong S, McCluskie K, Catley M, De Alba J, et al. Ikappa-B kinase-2 inhibitor blocks inflammation in human airway smooth muscle and a rat model of asthma. *Am J Respir Crit Care Med* 2005;172:962-971.
36. Rastelli G, Tian ZQ, Wang Z, Myles D, Liu Y. Structure-based design of 7-carbamate analogs of geldanamycin. *Bioorg Med Chem Lett* 2005;15:5016-5021.
37. Hertlein E, Wagner AJ, Jones J, Lin TS, Maddocks KJ, Towns WH 3rd, et al. 17-DMAG targets the nuclear factor-kappaB family of proteins to induce apoptosis in chronic lymphocytic leukemia: clinical implications of HSP90 inhibition. *Blood* 2010;116:45-53.
38. Xia Y, Yeddula N, Leblanc M, Ke E, Zhang Y, Oldfield E, et al. Reduced cell proliferation by IKK2 depletion in a mouse lung-cancer model. *Nat Cell Biol* 2012;14:257-265.
39. Di Stefano A, Caramori G, Oates T, Capelli A, Lusuardi M, Gnemmi I, et al. Increased expression of nuclear factor-kappaB in bronchial biopsies from smokers and patients with COPD. *Eur Respir J* 2002;20:556-563.

40. Franklin WA, Gazdar AF, Haney J, Wistuba II, La Rosa FG, Kennedy T, et al.
Widely dispersed p53 mutation in respiratory epithelium. A novel mechanism for field carcinogenesis. *J Clin Invest* 1997;100:2133-2137.
41. Schulze K, Imbeaud S, Letouzé E, Alexandrov LB, Calderaro J, Rebouissou S, et al.
Exome sequencing of hepatocellular carcinomas identifies new mutational signatures and potential therapeutic targets. *Nat Genet* 2015;47:505-511.
42. Cancer Genome Atlas Research Network. Comprehensive molecular profiling of lung adenocarcinoma. *Nature* 2014;511:543-550.
43. Sunwoo JB, Chen Z, Dong G, Yeh N, Crowl Bancroft C, Sausville E, et al. Novel proteasome inhibitor PS-341 inhibits activation of nuclear factor-kappa B, cell survival, tumor growth, and angiogenesis in squamous cell carcinoma. *Clin Cancer Res* 2001;7:1419-1428.
44. Lilenbaum R, Wang X, Gu L, Kirshner J, Lerro K, Vokes E. Randomized phase II trial of docetaxel plus cetuximab or docetaxel plus bortezomib in patients with advanced non-small-cell lung cancer and a performance status of 2: CALGB 30402. *J Clin Oncol* 2009;27:4487-4491.
45. McLoed AG, Sherrill TP, Cheng DS, Han W, Saxon JA, Gleaves LA, et al.
Neutrophil-Derived IL-1 β Impairs the Efficacy of NF- κ B Inhibitors against Lung Cancer. *Cell Rep* 2016;16:120-132.
46. Xue W, Meylan E, Oliver TG, Feldser DM, Winslow MM, Bronson R, et al.
Response and resistance to NF- κ B inhibitors in mouse models of lung adenocarcinoma. *Cancer Discov* 2011;1:236-47.

47. Van Waes C. Targeting NF- κ B in mouse models of lung adenocarcinoma. *Cancer Discov* 2011;1:200-202.
48. Ling J, Kang Y, Zhao R, Xia Q, Lee DF, Chang Z, Li J, et al. KrasG12D-induced IKK2/ β /NF- κ B activation by IL-1 α and p62 feedforward loops is required for development of pancreatic ductal adenocarcinoma. *Cancer Cell* 2012;21:105-120.
49. Daniluk J, Liu Y, Deng D, Chu J, Huang H, Gaiser S, et al. An NF- κ B pathway-mediated positive feedback loop amplifies Ras activity to pathological levels in mice. *J Clin Invest* 2012;122:1519-1528.
50. Travis WD, Brambilla E, Noguchi M, Nicholson AG, Geisinger KR, Yatabe Y, et al. International association for the study of lung cancer/american thoracic society/european respiratory society international multidisciplinary classification of lung adenocarcinoma. *J Thorac Oncol* 2011;6:244-285.

FIGURE LEGENDS

Figure 1. NF- κ B activation in urethane-induced lung adenocarcinoma. (A-F) *NGL* mice were backcrossed > F9 to the carcinogen- susceptible *FVB* strain and received single intraperitoneal injections of saline ($n = 6$) or the tobacco-contained carcinogen urethane (1 g/Kg; $n = 7$) and were imaged longitudinally for bioluminescence. **(A)** Legend to respiratory epithelial cells used in schematics throughout. **(B)** Schematic of experimental time-course (boxes = months) and topology of NF- κ B-reporter (green cytosol) versus *Kras*^{Q61R}-mutant (red nucleus) cells in this model. **(C)** Data summary of chest bioluminescence shown as mean (points), SEM (bars), and two-way ANOVA *P* value. * and ***: $P < 0.05$ and $P < 0.001$, respectively, for urethane- compared with saline-treated mice by Bonferroni post-tests. **(D)** Representative merged bioluminescent/photographic images with pseudocolor scale showing increased chest light emission of urethane-treated mice at early and late time- points after carcinogen injection (arrows). **(E)** Representative images of gross lungs and hematoxylin/eosin-stained lung sections of saline- and urethane-treated mice at eight months post-injection showing lung adenocarcinomas in the latter (arrows). **(F)** Light- optic and green fluorescent lung images of representative urethane-treated mouse at eight months post-injection showing NF- κ B-driven GFP expression in lung adenocarcinomas (dashed lines).

Figure 2. Increased NF- κ B activity and enhanced IKK α expression of *KRAS*- driven lung adenocarcinoma. (A, C, E) *FVB* mice ($n = 14$) received 1 g/Kg intraperitoneal urethane and were sacrificed after the indicated time intervals. **(B, D, F)** Mice carrying a conditional loxP-STOP-loxP.*KRAS*^{G12D} allele (*LSL.KRAS*^{G12D}; *C57BL/6* strain; $n = 12$) received 5×10^8 intratracheal PFU adenovirus encoding CRE (*Ad-Cre*) and were sacrificed after the indicated

time intervals. (A, B) Schematic representations of intensity and time-course of inflammation, hyperplasia, and tumorigenesis in the two models (8, 20-22, 25). (C, D) Immunoblots of whole lung nuclear and cytoplasmic extracts for NF- κ B pathway components. (C) Note the increased expression of *RelA*, *RelB*, *I κ B β* , *IKK α* , *IKK β* , and *TBK1* at late time-points post-urethane, when lung adenocarcinomas have developed. (D) Note the increased expression of *RelB*, *P52*, and *TBK1* at four months post-Ad-*Cre*, when lung adenocarcinomas have developed. (E) *FVB* mice ($n = 5$) received 1 g/Kg intraperitoneal urethane and were sacrificed after eight months for fluorescent detection of *IKK α* and *IKK β* immunoreactivity on cryosections of lungs with bronchi (b) and alveoli (a) and lung tumors (dashed lines). (F) *LSL.KRAS^{G12D}* mice (*C57BL/6* strain; $n = 5$) received 5×10^8 intratracheal PFU Ad-*Cre* and were sacrificed after four months for fluorescent detection of *IKK α* and *IKK β* immunoreactivity on cryosections of lungs with bronchi (b) and alveoli (a) and lung tumors (dashed lines). Note the increased immunoreactivity of lung adenocarcinomas for *IKK α* (arrows). *Rel*, v-rel avian reticuloendotheliosis viral oncogene homolog; *I κ B*, inhibitor of NF- κ B; *IKK*, inhibitor of NF- κ B kinase; *TBK*, TANK-binding kinase.

Figure 3. Adenoviral-mediated *IKK α* deletion from the respiratory epithelium protects *C57BL/6* mice from multi-hit urethane-induced lung adenocarcinoma. Conditional CRE-reporter (*mT/mG*) and *IKK α* (*Chukf/f*) or *IKK β* (*Ikkb/f/f*) gene-deleted mice (*C57BL/6* background) received 5×10^9 PFU intratracheal Ad-*Cre* followed by ten consecutive weekly intraperitoneal urethane injections (1 g/Kg) commenced two weeks post-Ad-*Cre* and were killed six months later. (A) Schematic of experimental time-course (boxes = months) and topology of *IKK*-deleted (pink cytosol) versus *Kras^{Q61R}*-mutant (red nucleus) cells in this model. (B) Kaplan-Meier plot of survival with log-rank *P* value. ns and *: $P > 0.05$ and $P <$

0.05, respectively, for the indicated comparisons by log-rank test. **(C)** Frequency distribution of lung tumors with n and χ^2 P value. ns and **: $P > 0.05$ and $P < 0.01$, respectively, for the indicated comparisons by Fischer's exact test. **(D-F)** Data summary of lung tumor number, mean diameter, and total volume (burden) per lung with raw data points (dots), Tukey's whiskers (boxes: interquartile range; bars: 50% extreme quartiles), and Kruskal-Wallis ANOVA P values. ns, *, **, and ***: $P > 0.05$, $P < 0.05$, $P < 0.01$, and $P < 0.001$, respectively, for the indicated comparisons by Dunn's post-tests. **(G)** Representative images of gross lungs. Arrows denote lung tumors.

Figure 4. IKK α deletion ameliorates respiratory epithelial oncogenicity of mutant

***KRAS*^{G12D}**. Conditional IKK α (*Chuk1ff*) or IKK β (*Ikk1b1ff*) gene-deleted mice were intercrossed with mice carrying a loxP-STOP-loxP.*KRAS*^{G12D} conditional allele (LSL.*KRAS*^{G12D}; all *C57BL/6*) and their offspring received 5×10^8 PFU intratracheal Ad-*Cre* and was killed four months later. **(A)** Schematic of experimental time-course (boxes= months) and topology of IKK-deleted (pink cytosol) versus *KRAS*^{G12D}-mutant (red nucleus) cells in this model, where IKK-deletion and oncogenic *KRAS*^{G12D} expression uniquely coincide in the same cells. **(B)** Frequency distribution of lung tumorigenesis with n and χ^2 P values. ns, *, **, and ***: $P > 0.05$, $P < 0.05$, $P < 0.01$, and $P < 0.001$, respectively, for the indicated comparisons by Fischer's exact test. **(C, D)** Data summary of relative lung tumor fraction and total lung tumor volume (burden) per lung with raw data points (dots), Tukey's whiskers (boxes: interquartile range; bars: 50% extreme quartiles), and Kruskal-Wallis ANOVA P values. ns, *, **, and ***: $P > 0.05$, $P < 0.05$, $P < 0.01$, and $P < 0.001$, respectively, for the indicated comparisons by Dunn's post-tests. **(E)** Representative hematoxylin and eosin-stained lung tissue sections. Arrows denote lung tumors.

Figure 5. IKK α selectively promotes the growth of KRAS-mutant cells *in vivo*. HEK293T cells were stably transfected with a constitutive luciferase reporter (pCAG.Luc), followed by plasmids encoding control random sequence (pC), wild-type (peGFP.Kras^{WT}) or mutant (peGFP.Kras^{G12C}) murine *Kras* in frame with eGFP, and murine IKK α (pChuk) or IKK β (pIkbbk) in various combinations. Two million cells were injected at different spots of the skin of *NOD/SCID* mice ($n = 16$) followed by serial spot volume assessment and bioluminescent imaging of spot cell mass. Mice were killed after six weeks for assessment of primary spots and lungs for tumorigenicity of the injected cells. **(A)** Schematic of *in vivo* competition studies between bioluminescent cells expressing combinations of peGFP.Kras^{WT}, peGFP.Kras^{G12C}, pChuk, and pIkbbk and representative bioluminescent images. **(B, C)** Data summary of spot bioluminescence (B) and volume (C) of pC (grey), pChuk (red), and pIkbbk (blue) -expressing cells shown as mean (points), SEM (bars), and two-way ANOVA *P* values. ns, *, and ***: $P > 0.05$, $P < 0.05$, and $P < 0.001$, respectively, for comparisons of the indicated color-matched data-points to pC-expressing cells at the same time-point by Bonferroni post-tests. **(D)** Representative lung images of mice carrying peGFP.Kras^{WT} (top) and peGFP.Kras^{G12C} (bottom) tumors showing lung metastases of luminescent cells in the latter. **(E)** Immunoblots of tumor nuclear and cytoplasmic extracts for NF- κ B pathway components. **(F)** IKK α and IKK β immunoreactivity of flank tumor cryosections showing increased immunoreactivity of peGFP.Kras^{G12C}/pChuk tumors for IKK α (arrows). *Rel*, v-rel avian reticuloendotheliosis viral oncogene homolog; IKK, inhibitor of NF- κ B kinase.

Figure 6. Dual blockade of IKK α and IKK β is effective against KRAS^{G12D}-driven lung adenocarcinoma *in vivo*. Mice harboring a conditional loxP-STOP-loxP.R26.Luc allele constitutively expressed in the ROSA locus (LSL.R26.Luc) were intercrossed with conditional

mice carrying a loxP-STOP-loxP.*KRAS*^{G12D} allele (LSL.*KRAS*^{G12D}; all *C57BL/6*). Double transgenic LSL.*KRAS*^{G12D};LSL.*R26.Luc* mice ($n = 30$) received 5×10^8 intratracheal PFU adenovirus encoding CRE (*Ad-Cre*) and were allocated to daily intraperitoneal treatment with the selective IKK β inhibitor TPCA-1 or the dual IKK α /IKK β inhibitor 17-DMAG (both at 0.5 mg/Kg in 100 μ L saline; approximately equivalent to 1-2 μ M by body volume extrapolation) before (prevention trial; days 14-28 post-*Ad-Cre*) or after (regression trial; days 84-112 post-*Ad-Cre*) lung adenocarcinoma establishment. Thereafter mice were imaged longitudinally for bioluminescence. **(A)** Topology of luminescent *R26.Luc* (green cytosol) versus *KRAS*^{G12D}-expressing (red nucleus) cells in this model. **(B)** Schematic of experimental time-course (boxes = weeks). **(C)** Data summary of chest bioluminescence shown as mean (points), SEM (bars), and two-way ANOVA *P* value. ** and ***: $P < 0.01$ and $P < 0.001$, respectively, for comparisons of the indicated data-points to saline-treated mice at the same time-point by Bonferroni post-tests. **(D)** Representative merged bioluminescent/photographic images with pseudocolor scale showing decreased chest (dashed lines) light emission of 17-DMAG-treated mice at 112 days post-*Ad-Cre*.

Figure 7. IKK α in human lung adenocarcinoma. **(A)** Data summary of normalized *CHUK* and *IKBKB* expression in tumor and adjacent normal-appearing lung tissues of 23 patients with lung cancer (43) by microarray. Data are shown as mean (columns), SEM (bars), raw data points (dots), and two-way repeated measures ANOVA *P* value. ns and ***: $P > 0.05$ and $P < 0.001$ for the indicated comparisons by Bonferroni post-tests. **(B)** Data summary of IKK α and IKK β immunoreactivity of tumor and adjacent normal- appearing lung tissues of 35 patients with lung cancer (43) by immunohistochemistry. Data are shown as mean (columns), SEM (bars), raw data points (dots), and two-way repeated measures ANOVA *P* value. ns, **, and

***: $P > 0.05$, $P < 0.01$, and $P < 0.001$ for the indicated comparisons by Bonferroni post-tests.

(C) Representative IKK α - and IKK β -immunostained lung and tumor tissue sections showing IKK α -immunoreactive cells (arrows). (D) Schematic of proposed role of IKK α in *KRAS*-mutant lung adenocarcinoma. Endogenous IKK α activity sporadically prevails over IKK β signalling across different cell types of the respiratory epithelium of smokers. Upon chemical induction of stochastic *KRAS* mutations across the respiratory field, pre-existing IKK α activity fosters the survival of *KRAS*-mutant cells and is therefore addicted to the oncogene, while IKK β signaling promotes the survival and maintenance of non-mutated cells and IKK β -dependent cells that suffer *KRAS*-mutations are destined to death. This opposing addiction of IKK α and IKK β to mutant and wild-type *KRAS*, respectively, leads over time to the appearance of *KRAS*-mutant lung adenocarcinomas with enhanced IKK α activity. (E) Summary of *in vivo* IKK deletion/targeting experiments shown as mean percentile reduction of lung tumor burden by IKK α and IKK β -targeted intervention (lines), SEM (bars), raw data (each dot represents one arm of an experiment), and paired Student's t-test P value.

Figure 1

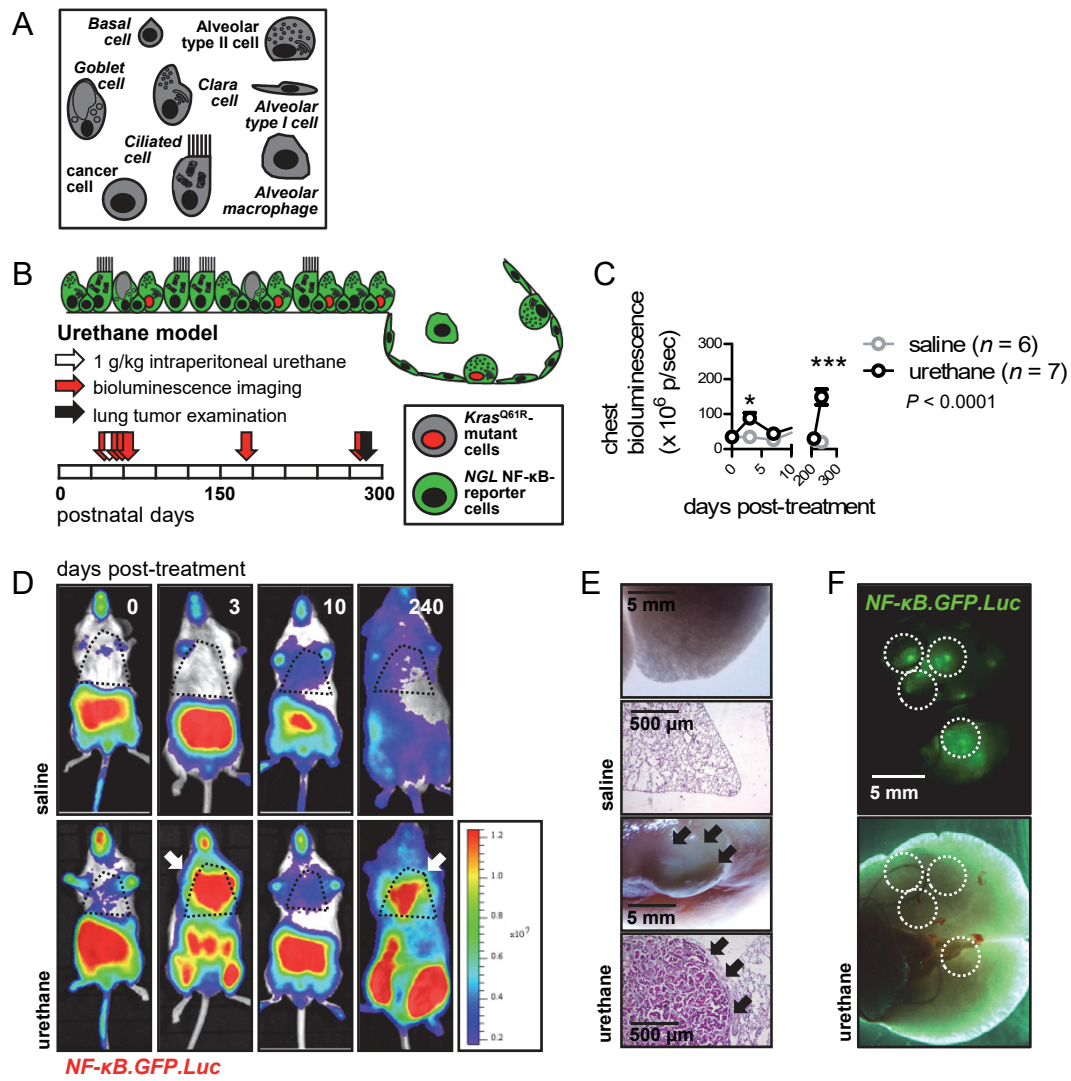


Figure 2

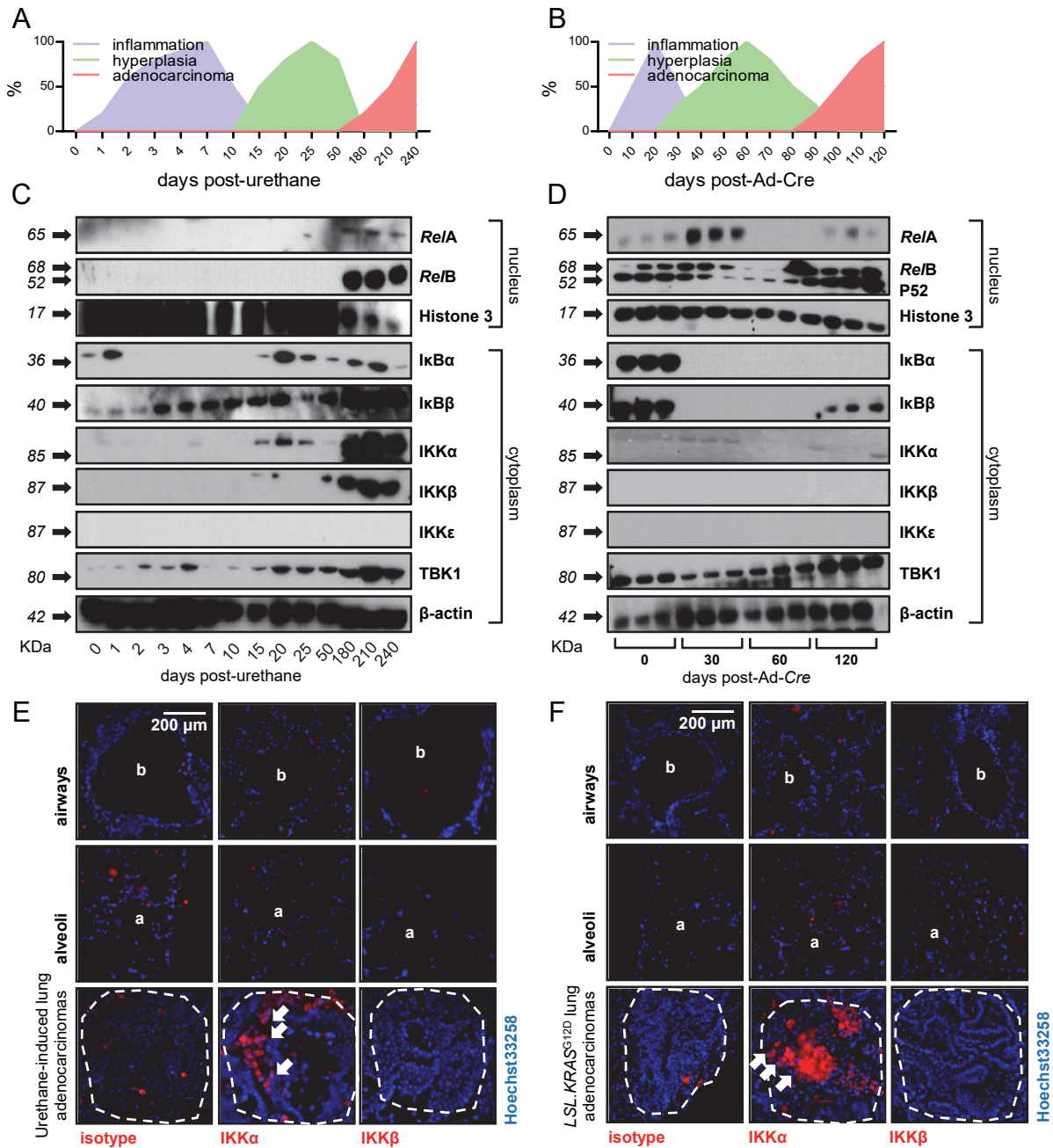


Figure 3

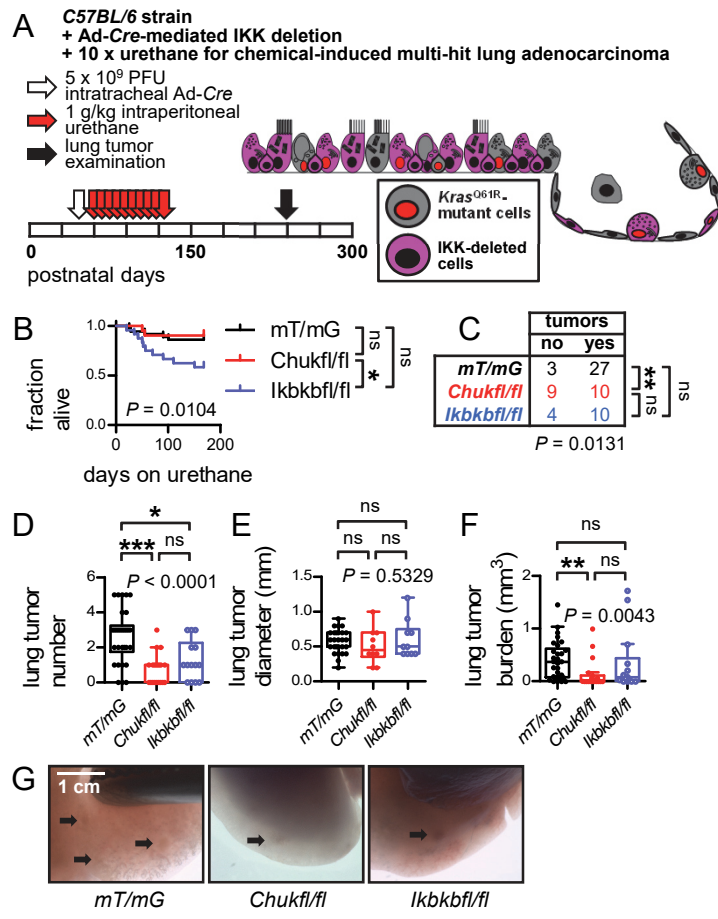


Figure 4

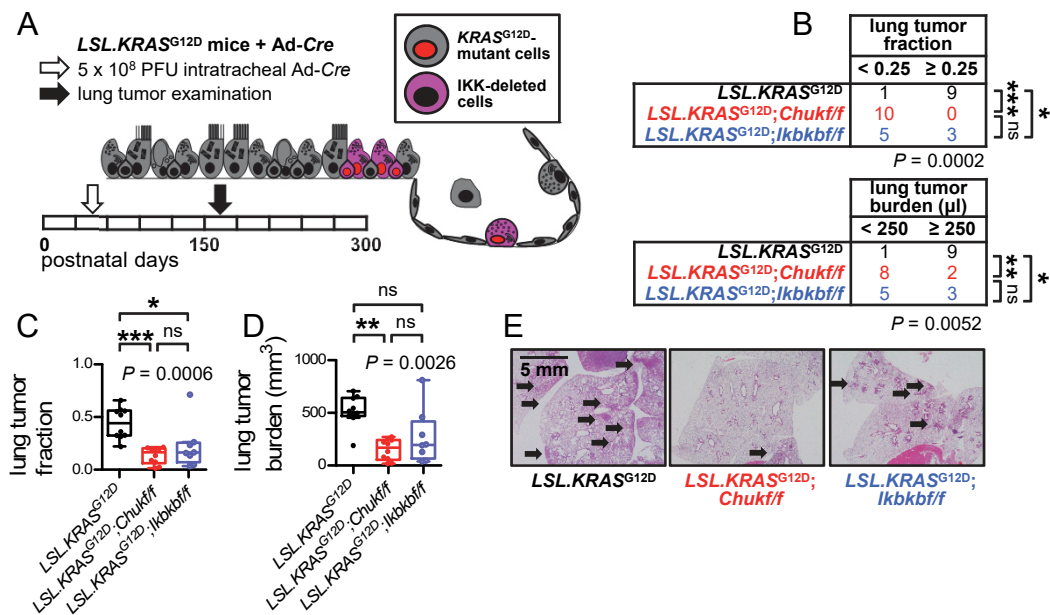


Figure 5

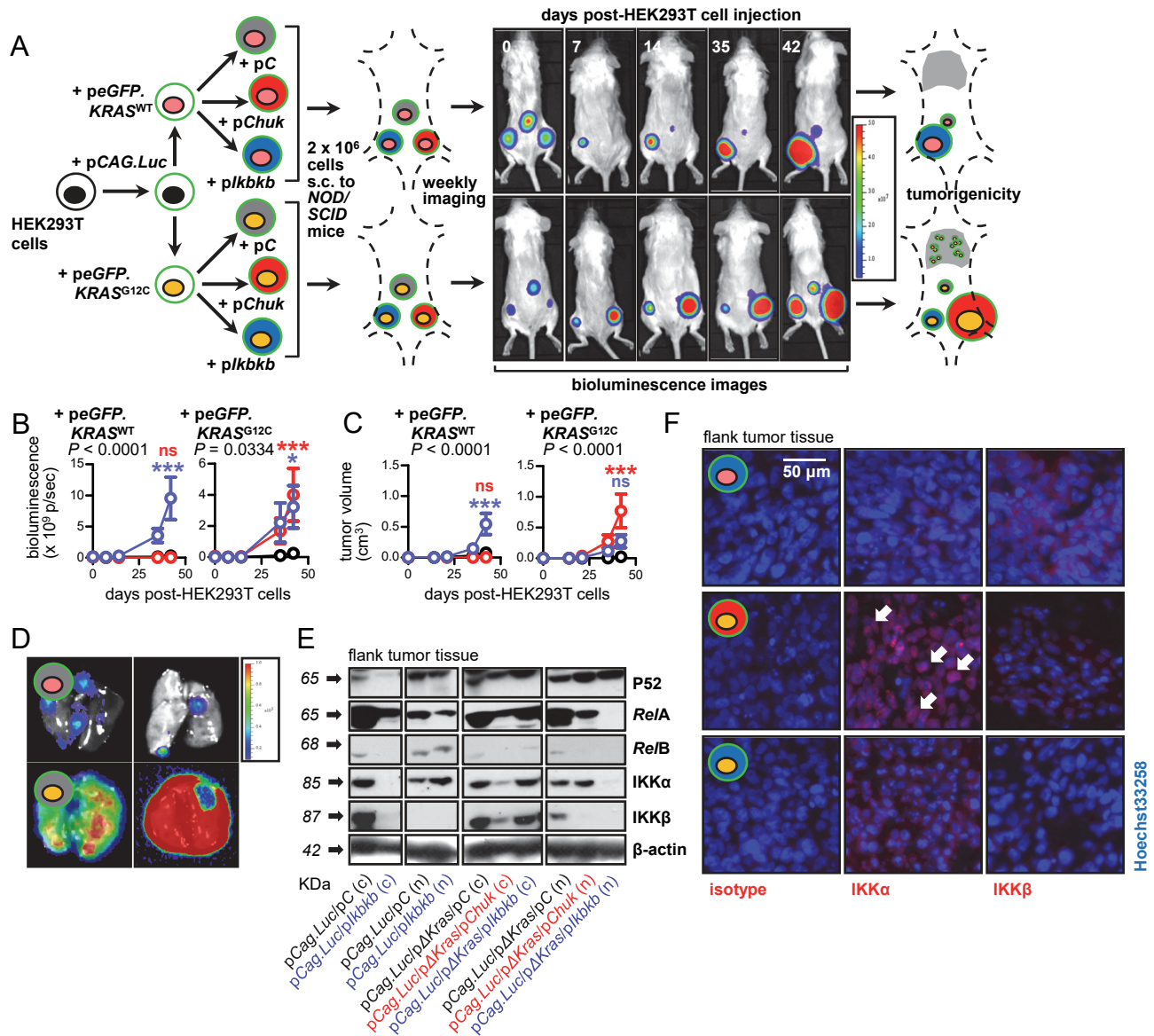


Figure 6

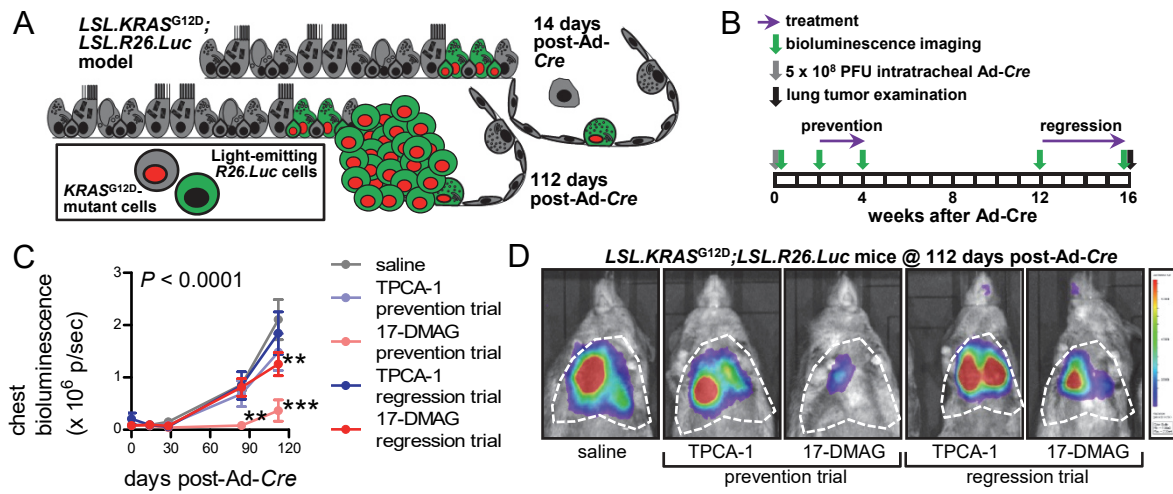
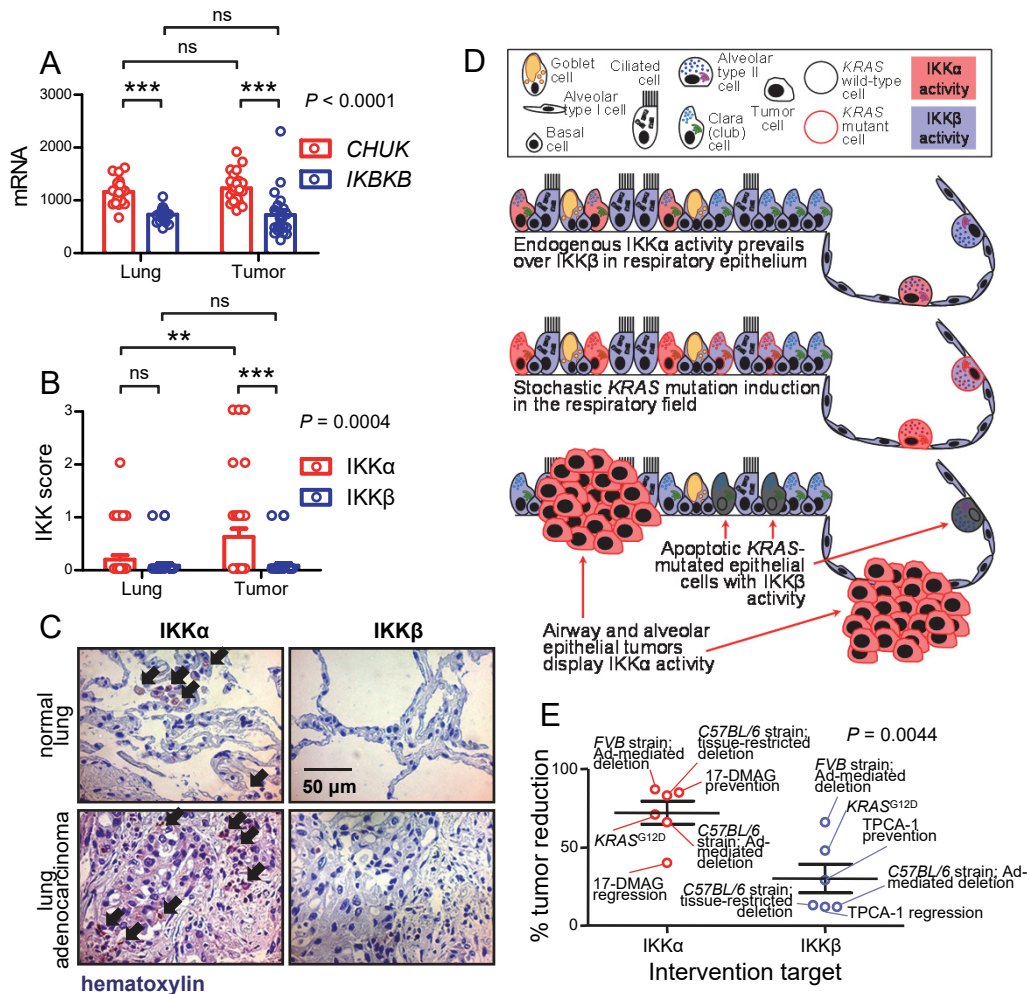


Figure 7



Cancer Research

The Journal of Cancer Research (1916–1930) | The American Journal of Cancer (1931–1940)

IK? kinase α is required for development and progression of KRAS-mutant lung adenocarcinoma.

Malamati Vreka, Ioannis Lilis, Maria Papageorgopoulou, et al.

Cancer Res Published OnlineFirst March 27, 2018.

Updated version	Access the most recent version of this article at: doi: 10.1158/0008-5472.CAN-17-1944
Supplementary Material	Access the most recent supplemental material at: http://cancerres.aacrjournals.org/content/suppl/2018/03/27/0008-5472.CAN-17-1944.DC1
Author Manuscript	Author manuscripts have been peer reviewed and accepted for publication but have not yet been edited.

E-mail alerts [Sign up to receive free email-alerts](#) related to this article or journal.

Reprints and Subscriptions To order reprints of this article or to subscribe to the journal, contact the AACR Publications Department at pubs@aacr.org.

Permissions To request permission to re-use all or part of this article, use this link <http://cancerres.aacrjournals.org/content/early/2018/03/27/0008-5472.CAN-17-1944>. Click on "Request Permissions" which will take you to the Copyright Clearance Center's (CCC) Rightslink site.